A Climatology of Atmospheric Wavenumber Spectra of Wind and Temperature Observed by Commercial Aircraft

G. D. NASTROM

Control Data Corporation, Minneapolis, MN 55440

K. S. GAGE

Aeronomy Laboratory, National Oceanic and Atmospheric Administration, Boulder, CO 80303

(Manuscript received 2 April 1984, in final form 4 December 1984)

ABSTRACT

Atmospheric wavenumber spectra of wind and temperature have been obtained from over 6000 commercial aircraft flights made during the Global Atmospheric Sampling Program. Temperature and velocity spectra are approximately the same shape over the range of wavelengths 2.6 to 10^4 km. Spectral slopes are close to $-5/3$ in the range 2.6 to 300–400 km and are independent of latitude, season and location in the troposphere or stratosphere. At larger scales, spectral slopes steepen considerably and approach -3. It is found that spectral amplitudes of wind and temperature have log-normal frequency distributions. Spectral amplitudes in the range 2.6 to 400 km vary somewhat with latitude, season and location in the troposphere or stratosphere. Temperature spectral magnitude varies more than velocity spectral magnitude, and is largest in the stratosphere and winter troposphere and smallest in the tropical troposphere. Meridional velocity spectral amplitude varies only slightly from the troposphere to the stratosphere but does show a significant variation with latitude being smallest in the tropics. Zonal velocity spectral amplitude varies with latitude considerably less than the meridional velocity spectral amplitude. The seasonal variation of spectral amplitude is about the same at midlatitudes for meridional and zonal velocities, with smallest values observed during summer.

1. Introduction

Recently, considerable attention has been focused on the distribution of atmospheric kinetic energy over the range of scales commonly referred to as the mesoscale. Conventional wisdom suggested a broad mesoscale gap in atmospheric kinetic energy. The existence of a gap was rationalized by Fiedler and Panofsky (1970) as the intermediate region between large-scale geostrophic turbulence with a steep k^{-3} spectral fall-off with a baroclinic energy source, and small-scale turbulence with a source at a scale of a few kilometers and inertial energy cascade through smaller scales. It is sometimes argued that the existence of a mesoscale gap in atmospheric spectra would favor the predictability of atmospheric motions at the larger synoptic scales. Certainly, the shape of the mesoscale spectra and the nature of nonlinear interactions responsible for these spectra are important considerations for atmospheric predictability over a range of scales.

As pointed out recently by Gage (1979), Lilly (1983) and Atkinson (1981), the atmospheric mesoscale possesses far more kinetic energy than is consistent with the concept of a broad mesoscale spectral gap, although the empirical basis for our understanding of atmospheric spectra on the mesoscale is still very sketchy. Large-scale frequency and wavenumber spectra are easily obtained from rawinsonde data but they give no information about the mesoscale. Recently, nearly continuous wind measurements have become available which enable the examination of atmospheric spectra over time scales ranging from a few minutes to many days (Balsley and Carter, 1982; Larsen *et al.*, 1982). However, single station measurements do not permit a direct examination of atmospheric wavenumber spectra. The latter have been inferred by assuming the spectra are due to turbulence and applying the Taylor transformation. Brown and Robinson (1979) established the validity of the Taylor transformation for scales in the range 500–1000 km by comparing frequency and wavenumber spectra over Eastern Europe. Lilly and Petersen (1983) and Nastrom and Gage (1983) presented spectral analysis results from a limited sample of aircraft data and showed that the wavenumber spectra of velocity was approximately the same as the Taylor transformed frequency spectra mentioned above.

Two mechanisms have been suggested to be responsible for the observed mesoscale spectra. The first is strongly nonlinear and can be categorized as quasi-two-dimensional turbulence which includes geostrophic turbulence (Charney, 1971) and stratified turbulence (Lilly, 1983). The second mechanism is

weakly nonlinear and involves a spectrum of internal buoyancy waves. The wave theory has been developed extensively by Garrett and Munk in a series of papers (for a brief introduction, see Garrett and Munk, 1979) and has been successfully applied to explain the observed structure of ocean spectra (Olbers, 1983). Dewan (1979) and VanZandt (1982) have suggested that the observed atmospheric spectra are also due to waves. To gain insight regarding the physical processes responsible for the mesoscale spectra, it is useful to examine their variability. In this paper we present the observed spectra and a study of their climatology. In a companion paper (Gage and Nastrom, 1985) we address the theoretical interpretation of these observations.

2. The GASP data set

The Global Atmospheric Sampling Program (Perkins, 1976; Papathakos and Briehl, 1981) was conducted by NASA to gather data near the tropopause on minor constituents and meteorological variables. Data were collected automatically on cassette tapes on specially instrumented Boeing 747 aircraft in routine commercial service, with most measurements made between about 9 and 14 km. Tropopause heights were later interpolated in space and time to each GASP data location from NMC gridded analyses.

The data collection phase of GASP lasted from 1975 to 1979, and all data are available on magnetic tape from the National Climatic Center, Asheville, North Carolina. There are over 6900 flights in the GASP data set, made during all seasons and covering a wide variety of latitudes and longitudes. The flights are distributed evenly among months and about 80% of the data are from between 30°N and 55°N. The geographic distribution of data is illustrated in Fig. 1, which shows data density on a 6° longitude by 3° latitude grid. Observations from those flight segments at least 2400 km long and with nominal spacing of 75 km (explained later) were used in Fig. 1. A complete list of GASP routes is given in Nastrom and Jasperson (1983).

Wind data were taken from the onboard computer linked with the inertial navigation system and were recorded to the nearest knot (about 0.5 m s^{-1}) and degree. These winds have an uncertainty of about five percent of the reported value, due largely to inaccuracies in the true air speed measurement. They also have a sinusoidal (Schuler) error of period 84 minutes and random amplitude from 0 to 2.5 m s^{-1}, which arises from electronic tuning of the gyroscopes and accelerometers. The spectra to be presented below show no evidence of this effect. It was found that the wind direction data also have an apparently spurious periodicity near 30 sec period (near 8 km wavelength at an airspeed of 250 m s^{-1}). This effect leads to a local peak in the kinetic energy spectrum; this peak will show up in results presented below. When only flights oriented north–south were used,

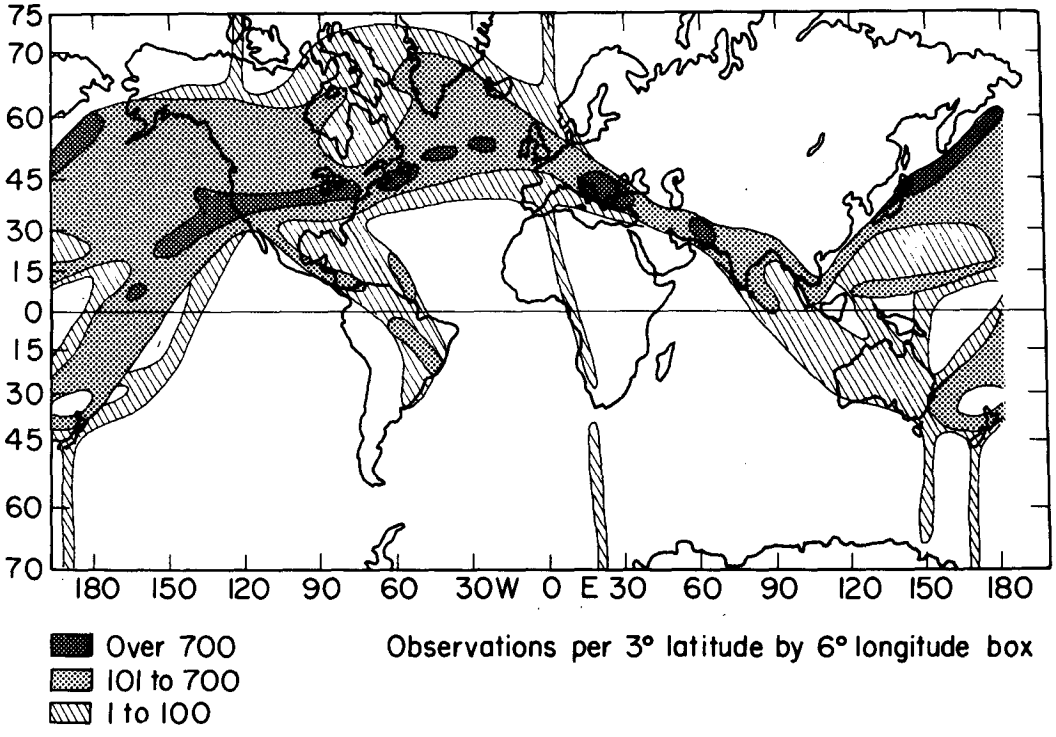

FIG. 1. Geographical distribution of GASP observations from flight segments at least 2400 km long; see text.

the peak was very strong in the zonal wind and nearly absent in the meridional wind; when only east–west flights were used, the reverse occurred, and for flights oriented diagonally with respect to latitude, both wind components shared a peak in their spectra. Thus, we conclude this peak is spurious; likely induced by the measurement platform. (The inertial navigation platform rotates at about one revolution per minute; thus any small inaccuracy, such as might be caused by sideslip, will appear in the wind records with a 30 second period. For geometrical reasons, the effect is most noticeable in the cross flight-path component.)

Temperatures were measured with a Rosemount temperature sensor for which the rms error is less than 1°C (Stickney *et al.* 1981) and the relative error from one observation to the next is a few tenths of a degree. The temperature data were recorded in whole degrees Celsius. Potential temperatures were computed prior to further analysis by using the recorded temperature and flight level pressure data. Actually, the spectral analyses were made using both temperature and potential temperature. As the results were similar, we have chosen to present only the results for potential temperature for the sake of brevity, although both variables have small shortcomings. The aircraft tend to bob up and down as much as a few tens of meters with a period of about twenty minutes (wavelength near 300 km), as illustrated by the average spectra of aircraft altitude in Fig. 2. In the troposphere where the vertical gradient of temperature is large, this bobbing introduces some spurious energy at high frequencies (short wavelengths), as implied by the cospectra in the lower part of Fig. 2. Potential temperature is less affected by this small bobbing, at least in the troposphere; but has the disadvantage that any errors in pressure measurement add to the errors in temperature measurement. As the relative error of the pressure measurement is less than 10 Pa, the relative error in potential temperature is less than one degree. To correct for this bobbing effect would require detailed knowledge of the local temperature gradient, which was not available for this study, thus no attempt has been made to normalize the temperature data, although we are considering ways to estimate the effect of bobbing on the temperature spectra.

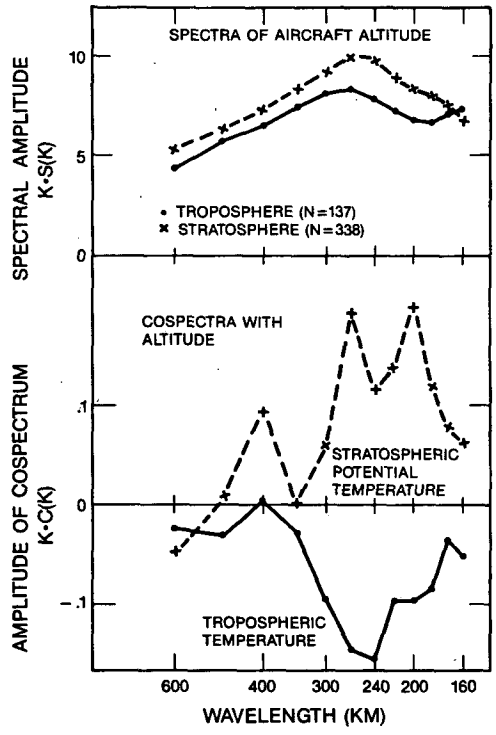

FIG. 2. Average spectra of aircraft altitude in the troposphere and stratosphere (upper). Cospectrum of altitude and temperature and potential temperature (lower). Relative units.

3. Analysis and results

First, we consider the spectra of wind and temperature over the widest span of wavelengths possible from the GASP data, 2.6 to 10^4 km. Nastrom *et al.* (1984), have presented the spectra for the wind components and their results are shown in Fig. 3. Also given in Fig. 3 is the spectrum of potential temperature, prepared using the same flights and method of analysis used for the wind components.

The GASP data were recorded under two modes, and the curves in Fig. 3 were prepared in two stages. On most flights, the GASP system was set to record data every five minutes (75 km intervals at an airspeed of 250 ms^{-1}). There were 311 flights that were over 10^4 km long and had an average orientation of east–west. Throughout this study we have used the common assumption that the speed of the airplane is much greater than the speed of movement of atmospheric disturbances. Zonal and meridional wind speeds and potential temperatures were interpolated to 75 km intervals along the flight path, the means and linear trends were removed from the data, a Fast Fourier Transform was applied to the residuals, and the sums of the squares of the Fourier components at each wavelength were averaged over all flights and plotted in Fig. 3. If two consecutive observations were missing on a flight, then that flight was not used. On long flights, the aircraft typically change cruise altitude every three or four hours, climbing about 600 m as fuel is burned. The last segment of the flight is thus about 1.2 km higher than the first on very long flights. For the wind components, we could detect no discontinuity between segments, so we used the wind data as reported. For potential temperature, however, there was usually a large discontinuity between segments. In an effort to remove these discontinuities, the last two observations of one leg were averaged and the first two observations of the next leg were averaged; the difference between the two averages was

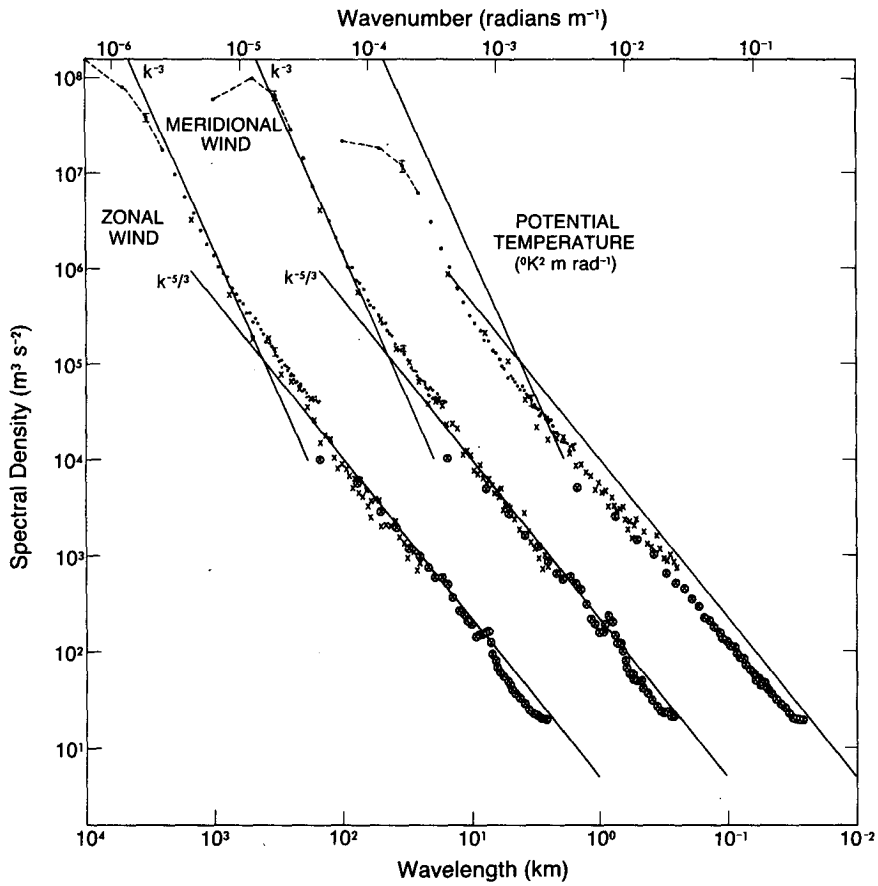

FIG. 3. Variance power spectra of wind and potential temperature near the tropopause from GASP aircraft data. The spectra for meridional wind and temperature are shifted one and two decades to the right, respectively; lines with slopes -3 and $-5/3$ are entered at the same relative coordinates for each variable for comparison.

then subtracted from all observations on the next leg. The analysis was then made using the normalized temperature data.

On selected flights the GASP system was set to record data at 4-second (about 1 km) intervals, rather than at 5-minute intervals. Data from the 97 high density recording flights were analyzed as segments. Each segment was 150 km long; if over five data points were missing during any minute, that segment was not used. Also, if the altitude changed more than 100 m along a segment, then that segment was not used. There were 1492 segments retained for analysis and the average latitude of these data is about 30°N. For each variable on each segment, the mean and a linear trend were removed, and then the Fast Fourier Transform was applied. The results over all segments were averaged and plotted in Fig. 3.

Standard deviations of the results in Fig. 3 are about the same magnitude as the mean values. The error bars are plotted to extend above and below the mean two times the standard deviation divided by the square root of the number of flights used to form the mean.

At the very longest wavelengths, spectra in Fig. 3 show a relatively small negative slope for zonal wind and temperature and a positive slope for meridional wind. This is characteristic of planetary scale waves as discussed at length by Boer and Shepherd (1983). Between about 1000 and 3000 km wavelength, all three spectra have a slope near -3. Lines with slopes -3 and $-5/3$ are entered at the same coordinates for all variables for comparison. The -3 slope is interpreted to imply an enstrophy cascade from longer to shorter wavelengths in quasi-geostrophic turbulence (Charney, 1971). At wavelengths below about 400 km, the spectra appear to follow a $-5/3$ slope. The magnitudes and general shapes of the spectra in Fig. 3 agree well with available past results for wind as illustrated in Fig. 4.

The potential temperature spectrum contained in Fig. 3 is the first temperature spectrum obtained over this range of scales. The relationship of the temperature spectrum to the velocity spectra is discussed at length in Gage and Nastrom (1985). Here we simply point out that the temperature spectrum parallels the velocity spectra at least down to the scales ($\leq$300

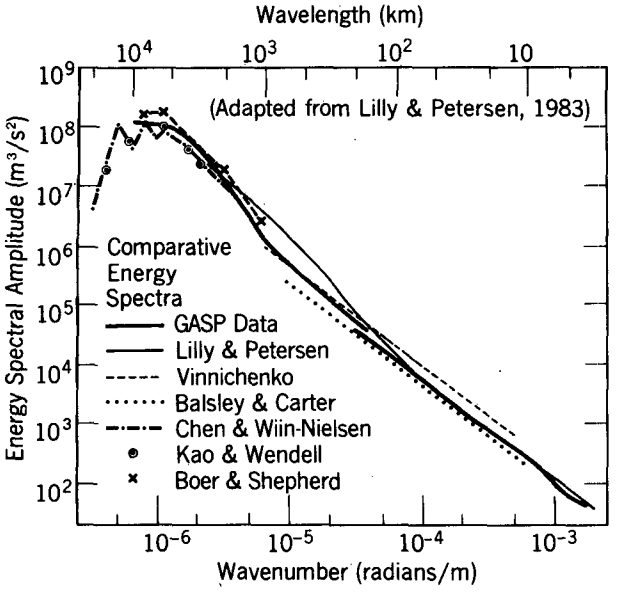

FIG. 4. Composite horizontal energy spectra with comparative results from Vinnichenko (1970), Balsley and Carter (1982), Chen and Wiin-Nielsen (1978), Kao and Wendell (1970), and Boer and Shepherd (1983) (adapted from Lilly and Petersen, 1983).

km) affected by the bobbing described above. Because of the bobbing, the potential temperature spectral amplitude is thought to be somewhat enhanced at the smallest scales.

There is no evidence of a broad mesoscale gap in the spectra in Fig. 3. Indeed, except for the instrument induced small peaks in the wind spectra near 8 km wavelength, they are all remarkably smooth and continuous over their entire spans. There is some evidence of aliasing by the unresolved high frequency motions at the short wavelength end of each portion of the spectra; i.e., the slopes approach zero at the right-hand end of each portion. Another feature, the apparent low energy of the short wavelength portions of 150 km wavelength, is due to the filtering effects of the linear trends. To help illustrate the blending of the short and long portions of the spectra, we analyzed all available segments of the continuous recording flights which were at least 1500 km long and which met our criteria described earlier for the 150 km segments. There were 39 segments that met all these criteria, and the results obtained from them are plotted as bold crosses in Fig. 3 over the wavelength span 25–1500 km. The crosses appear to blend smoothly with the short-wavelength portions (the circles), as well as with the long-wavelength portions (the dots). Any small differences may be ascribed to sampling fluctuations or to the difference in latitude (30°N versus 50°N) of the data used for the short and long wavelength portions of the spectra.

All available data were used to prepare Fig. 3, with no regard given to latitude, season, distance from the tropopause, etc. Stratifications of the data with respect to these factors will be presented next. For the short wavelength portion of the spectra we will continue to use the 1492 segments used above. At wavelengths greater than 150 km, however, we found it desirable to expand our data base beyond the 311 very long flights used above. This was done by reducing the maximum wavelength from 10^4 to 2400 km. All flight segments at least 2400 km long on which the altitude changed by less than 300 m, the tropopause was not crossed, and no two consecutive observations

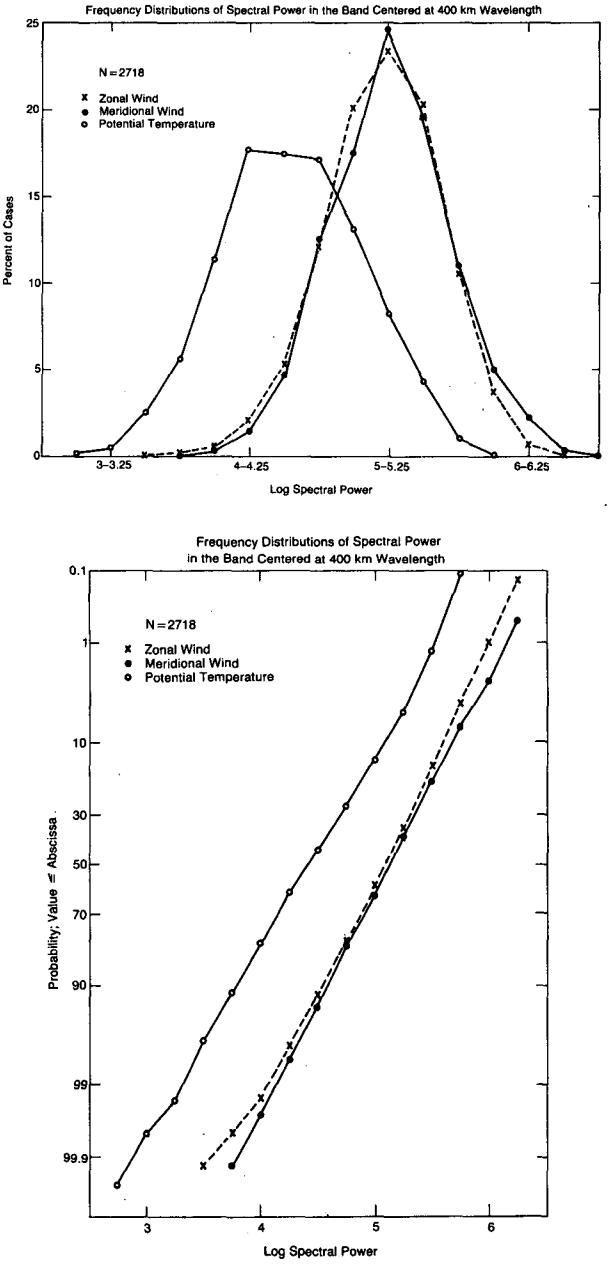

FIG. 5. Frequency distributions of spectral power in the band centered at 400 km wavelength. Upper: histogram coordinates; lower: cumulative probability coordinates.

were missing were analyzed as described above. There were 2718 segments which met these criteria.

This significantly expanded number of flight segments can be used to examine the empirical frequency distribution of spectral power at mesoscale wavelengths. Figure 5 shows the frequency distributions of the spectral power in the band centered at 400 km wavelength, as a typical example, for zonal and meridional winds and potential temperature. The upper panel is plotted in standard histogram format, with the logarithm of spectral power used along the abscissa. Noteworthy features are the apparently log-normal distributions of all three variables, the close correspondence of the curves for zonal and meridional wind, and the slightly flattened shape of the temperature distribution.

To further check these features, the same data have been plotted in probability coordinates in the lower panel of Fig. 5. These coordinates are designed so that a normal distribution will appear as a straight line, the mean is given by the 50 percent intercept, and the standard deviation is inversely related to the slope of the lines. In the figure, the plotted data very nearly fall on a straight line for all three variables, the curves for the two wind components are very similar, and the slope of the temperature curve is slightly smaller than those for wind. (The standard deviations for zonal and meridional wind and temperature are 0.41, 0.43, and 0.52, respectively.) It will be our goal in the following sections to see if some of the variability implied by these frequency distributions can be explained by variations with latitude, season, or distance from the tropopause.

a. Troposphere–stratosphere differences

The spectra of wind and potential temperature in the troposphere and stratosphere are given in Fig. 6. Only flight segments whose average latitude was between 25°N and 50°N were used here. Spectral amplitudes are larger in the stratosphere than in the troposphere at all wavelengths between about 4–800 km for zonal wind, and for all wavelengths less than about 500 km for meridional wind, except near the instrumentally induced peak near 8 km wavelength. The differences at most of these wavelengths are statistically significant at the five percent level by Student's-t test. Stratospheric values appear typically 1.2–1.5 times larger than tropospheric values, although some of this difference is due to the higher average

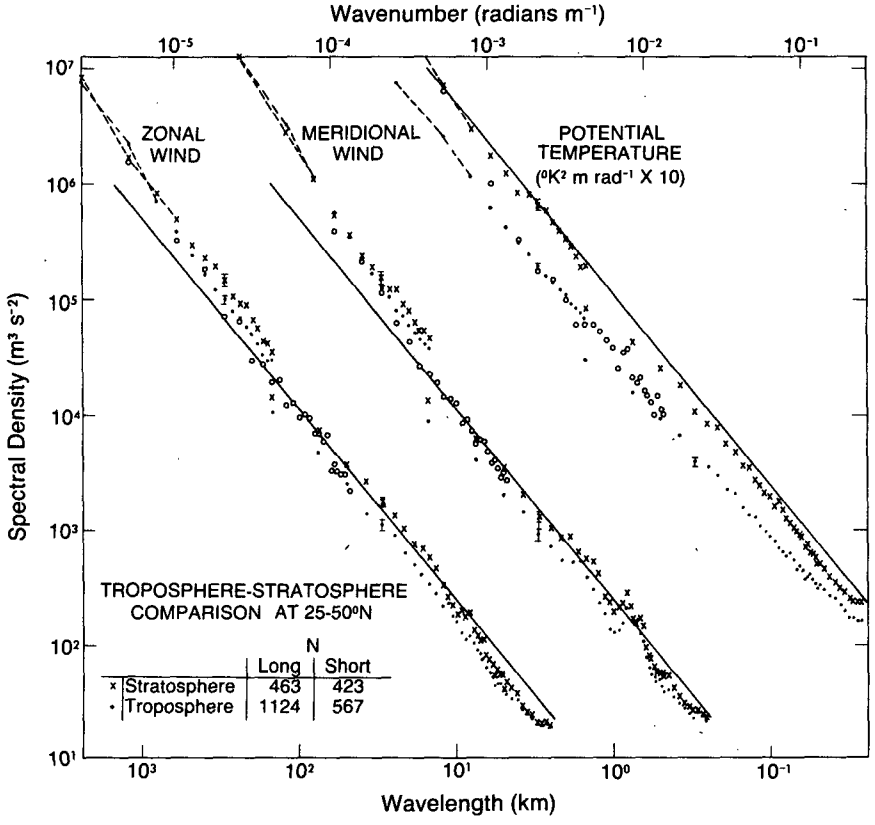

FIG. 6. Comparison of variance power spectra for flight segments in the troposphere and in the stratosphere, 25–50°N.

latitude of the stratospheric data, and the general increase of spectral amplitude with latitude, discussed in Section 3c.

For potential temperature, the stratospheric values are larger at all wavelengths, ranging from a factor of 4 at 2400 km wavelength to about 1.5 near 3 km wavelength. Most of this difference can be attributed to the change in stability across the tropopause. As discussed in detail in Gage and Nastrom (1985), the amplitude of the potential temperature spectrum is determined by the product of the vertical displacement spectrum and the potential temperature gradient squared. The effect of the larger stability in the stratosphere more than compensates for any decreased amplitude of the displacement spectrum in the stratosphere, resulting in increased amplitude of the stratospheric potential temperature spectrum. It is the shift in the mean spectral power across the tropopause which gives rise to the slightly flattened appearance of the frequency distribution for temperature in Fig. 5.

b. *Seasonal differences*

Tropospheric spectra are given by season in Fig. 7 for flights whose average latitude was between 25°N and 50°N. There were not enough flights to make a similar comparison in the stratosphere. In general, values are smaller during summer than other seasons for all three spectra and for all wavelengths. There is no clear pattern of any one season having largest values, except for the potential temperature spectra where winter is largest at nearly all wavelengths. We can ascribe this seasonal difference in potential temperature to changes in background static stability, as discussed further by Gage and Nastrom (1985). At planetary and synoptic scales, studies with balloon data have shown a distinct seasonal difference, with spectral amplitudes larger in winter than in summer (e.g., Kao and Wendell, 1970; Boer and Shepherd, 1983), consistent with our results.

c. *Latitude differences*

Tropospheric spectra of wind and temperature for wavelengths 150–2400 km and for latitudes 30°S–60°N are given in Fig. 8. There were not a sufficient number of flight segments in the stratosphere to prepare a corresponding stratospheric chart, nor were there enough 150 km segments at low latitudes to permit a meaningful comparison of short wavelength results. In Fig. 8, spectra for the tropical latitudes 0–

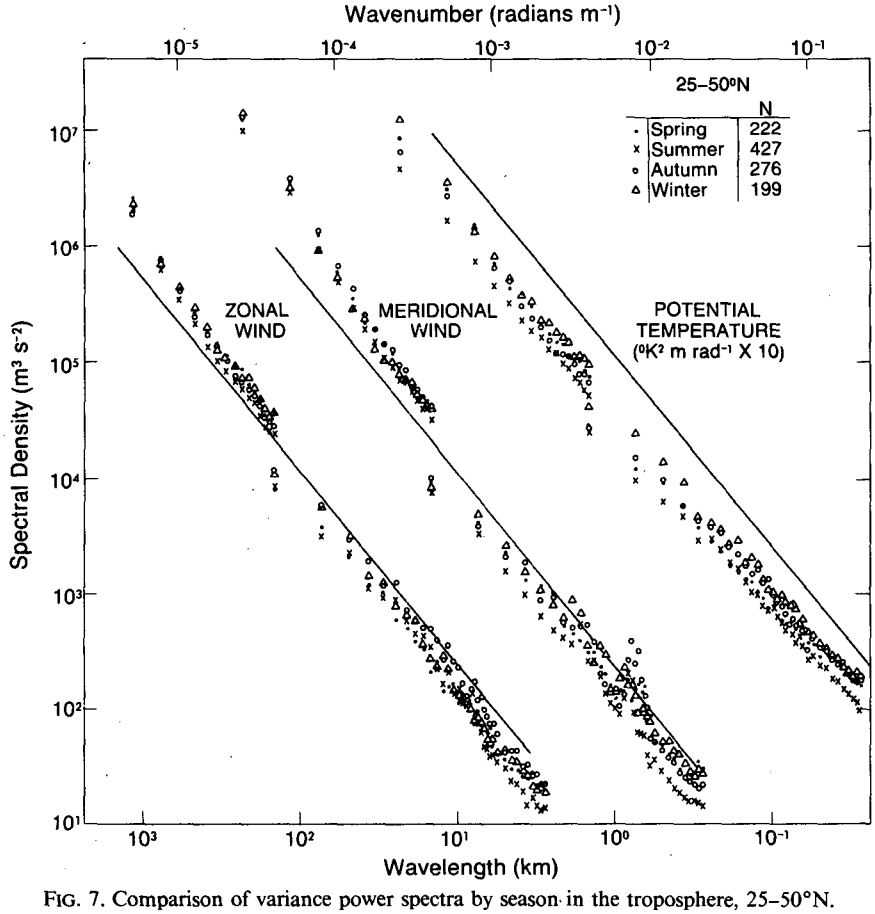

FIG. 7. Comparison of variance power spectra by season in the troposphere, 25–50°N.

15°S and 0–15°N usually have the lowest amplitudes (at least for wavelengths below about 10^3 km), and spectra for 45–60°N are the largest at nearly all wavelengths. The general impression from this figure is that amplitude gradually increases with latitude. Certainly, some variation with latitude should be expected because of the more vigorous nature of the baroclinic zone at midlatitudes. However, results from analyses of balloon data (e.g., Kao and Wendell, 1970) indicate the peak energy of synoptic-scale waves occurs near 40°N rather than at 60°N as seen in Fig. 8. Another possible explanation for the variation with latitude is that we have plotted our spectra as functions of wavelength, or wavenumber in rad m^{-1}. Large scale atmospheric disturbances often extend across a broad band of latitudes, and their spectra are often presented as functions of zonal wavenumber (Tang and Orszag, 1978) to take account of the decreasing distance around a circle of latitude as the pole is approached. This geometrical effect does indeed help normalize our results (Gage and Nastrom, 1985), so that differences with respect to latitude can be largely accommodated, although a notable exception to this explanation is the relatively very large amplitude of the spectrum of meridional wind at 45–60°N. An open question, also discussed in the companion paper, is "why does zonal wavenumber influence the spectral amplitude at scales of only a few hundred km?"

The amplitude of the tropical temperature spectra at long wavelengths in Fig. 8 is relatively very small compared with higher latitude results. As this feature seems part of a trend with latitude, we conclude that it is not due to a sampling problem, and is a genuine atmospheric signature. At wavelengths below about 300 km, on the other hand, the tropical values are more similar to those for other latitudes. This feature may be an artifact of the data, perhaps caused by the vertical bobbing of the aircraft at wavelengths near 300 km discussed earlier. That is, the variance induced by bobbing may be significant in the tropics compared with the atmospheric variance. Thus, the slope of the temperature spectrum in the tropics at wavelengths less than about 300 km should not be deduced from these results.

4. Summary

The results of the spectral analysis given here confirm and expand upon past studies of the spectra of mesoscale motions near the tropopause. The shapes of the spectra of wind and temperature show remarkably little variability with respect to any of the data stratification schemes used. At wavelengths below a few hundred km the spectrum has a slope near $-5/3$; the slope steepens to about -3 in the wavelength range 1000–3000 km.

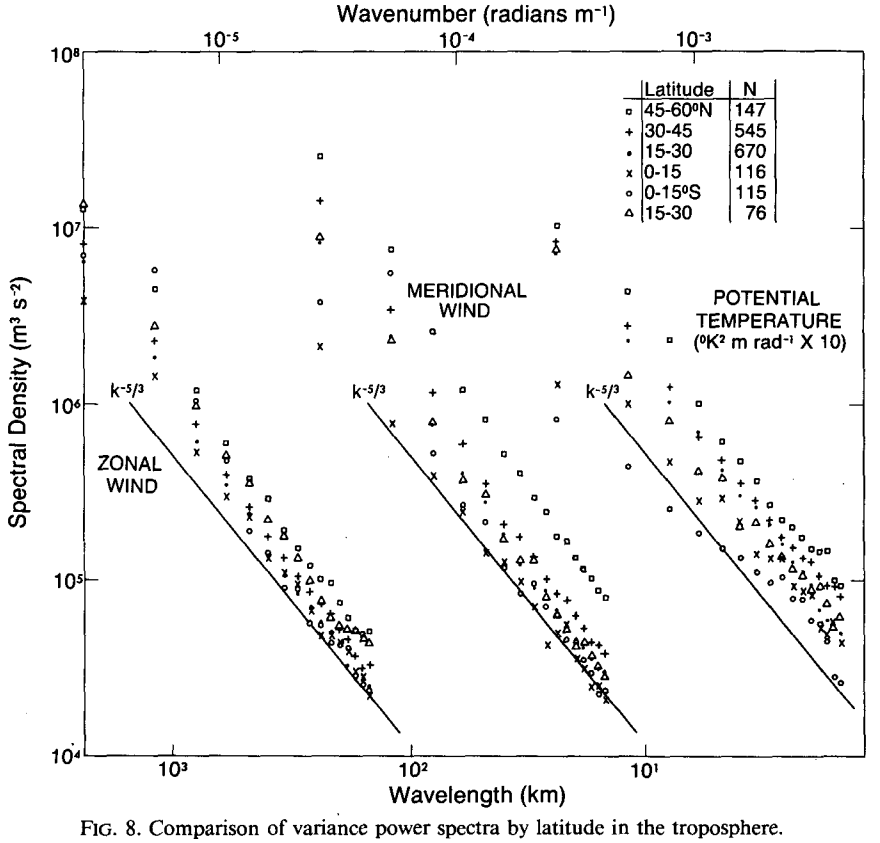

FIG. 8. Comparison of variance power spectra by latitude in the troposphere.

The amplitudes of the spectra also show a remarkably small variability with respect to different stratification schemes, with differences usually less than a factor of three or so. An exception is the difference in temperature amplitude between the troposphere and stratosphere, and this can be attributed to the difference in static stability across the tropopause. The spectra have been given on several graphs, and even though reference lines are included on the graphs, it may not be easy to detect similarities or differences among the amplitudes of the various stratifications. To help aid comparisons, Table 1 lists the integrated variance under the spectrum for wavelengths from 150–400 km for flight segments 2400 km long (Table 1a) and 1200 km long (Table 1b) and Table 2 lists the values for wavelengths from 12.5–25 km. The five percent confidence limit for each variance entry in the tables is approximately twice the value of the entry divided by the square root of the number of flights. The average latitude and scalar wind speed is given for each group in the tables. Note that the two sections of Table 1 present independent data. Thus, while most of the patterns with respect to latitude, season, or across the tropopause found in one section of the table are confirmed by the patterns in the other section, there are occa-

TABLE 1. Variance under the spectrum at 150–400 km wavelength.

	Troposphere						Stratosphere					
Group	N	Latitude (°N)	Wind speed (m s^{-1})	u	v	θ	N	Latitude (°N)	Wind speed (m s^{-1})	u	v	θ
(a) For flight segments 2400 km long												
All flights	1671	26	24	2.03	2.51	0.41	1047	50	24	2.60	2.81	1.24
Over 30 mb from the tropopause	1139	21	21	1.70	2.07	0.29	550	52	22	2.31	2.32	1.17
Over land	244	31	25	2.43	2.94	0.46	201	47	25	2.93	3.24	1.41
Over ocean	965	26	24	1.98	2.50	0.43	597	50	26	2.42	2.73	1.18
Eastbound	155	39	36	2.33	3.50	0.53	256	48	31	2.67	3.15	1.30
Westbound	225	34	23	1.96	2.69	0.44	140	50	20	2.58	3.20	1.39
>60°N	0						159	63	16	1.89	2.03	1.13
45–60	147	50	32	3.22	6.01	0.60	586	53	23	2.64	2.79	1.24
30–45	545	36	27	2.17	2.64	0.47	256	40	32	3.12	3.55	1.38
15–30	670	26	23	1.71	2.01	0.38	42	28	23	1.55	1.66	0.71
0–15	116	9	13	1.72	1.50	0.28	0					
0–15°S	115	−8	12	1.66	1.63	0.21	0					
15–30	76	−22	26	2.62	2.08	0.34	0					
<30°S	0						3					
Winter (at 25–50°N)	199	31	38	2.31	2.54	0.55	177	41	31	2.90	2.84	1.41
Spring	222	33	26	2.31	2.84	0.48	168	40	28	2.80	3.25	1.29
Summer	427	34	21	1.70	2.31	0.33	44	47	26	2.96	3.58	1.19
Autumn	276	35	24	2.08	2.99	0.41	74	46	37	2.79	3.51	1.05
(b) For flight segments 1200 km long												
All flights	2141	23	24	2.22	2.69	0.41	1297	47	25	2.72	2.79	1.30
Over 30 mb from the tropopause	1578	19	21	2.06	2.33	0.32	724	49	23	2.50	2.39	1.20
Over land	616	31	25	2.47	3.16	0.53	453	45	26	3.13	3.21	1.53
Over ocean	954	24	26	2.07	2.62	0.37	662	49	26	2.44	2.56	1.14
Eastbound	273	28	29	2.09	3.16	0.47	274	43	30	3.03	2.98	1.41
Westbound	359	28	23	2.15	3.28	0.50	324	47	23	2.82	2.95	1.45
>60°N	6						159	64	17	2.17	2.16	1.25
45–60	182	49	31	3.14	4.44	0.56	593	52	23	2.55	2.75	1.21
30–45	739	38	29	2.27	3.19	0.53	487	40	30	3.16	3.12	1.49
15–30	572	24	24	1.86	2.12	0.35	35	26	30	1.87	2.04	0.55
0–15	395	9	13	2.05	1.94	0.25	6					
0–15°S	70	−7	11	1.86	1.88	0.21	0					
15–30	117	−25	30	2.64	2.03	0.35	0					
<30°S	58	−36	26	2.69	3.08	0.54	17	−36	31	3.27	2.07	1.43
Winter (at 25–50°N)	163	34	43	2.41	2.98	0.66	250	41	31	3.06	2.80	1.43
Spring	247	36	30	2.68	3.71	0.53	278	41	27	3.28	3.39	1.57
Summer	415	37	23	2.12	3.15	0.45	77	44	25	2.23	2.76	1.08
Autumn	300	38	29	2.20	2.61	0.46	139	45	34	2.88	3.45	1.26

TABLE 2. Variance under the spectrum at 12.5–25 km wavelength.

	Troposphere						Stratosphere					
Group	N	Lat (°N)	Wind speed (m s^{-1})	u	v	θ	N	Lat (°N)	Wind speed (m s^{-1})	u	v	θ
All flights	844	27	30	0.132	0.130	0.058	634	34	28	0.200	0.188	0.145
Over ocean	497	24	29	0.100	0.110	0.042	244	34	31	0.147	0.168	0.116
Over land	335	32	32	0.180	0.161	0.083	387	39	27	0.232	0.200	0.163
Western U.S.	117	39	20	0.254	0.241	0.111	72	38	26	0.558	0.395	0.342
East–west	431	36	32	0.138	0.137	0.068	329	38	34	0.228	0.202	0.153
North–south	29	33	26	0.198	0.135	0.046	10	44	21	0.298	0.193	0.212
>60°N	6	62	13	0.148	0.094	0.057	52	72	16	0.116	0.118	0.095
45–60	42	50	39	0.088	0.148	0.042	144	53	26	0.183	0.187	0.136
30–45	401	38	32	0.159	0.156	0.077	359	38	33	0.224	0.202	0.157
15–30	252	26	32	0.100	0.101	0.043	19	27	36	0.188	0.109	0.125
0–15	46	7	11	0.155	0.118	0.033	0					
0–15°S	39	−8	9	0.115	0.097	0.021	0					
15–30	41	−22	36	0.089	0.102	0.040	0					
>30°S	17	−38	40	0.137	0.108	0.078	60	−65	16	0.169	0.184	0.145
Winter (at 25–50°N)	174	33	51	0.135	0.169	0.081	213	38	37	0.201	0.201	0.138
Spring	121	35	31	0.103	0.125	0.052	123	37	29	0.215	0.185	0.160
Summer	142	36	24	0.131	0.110	0.053	24	44	22	0.435	0.305	0.212
Autumn	157	36	22	0.180	0.156	0.072	36	41	25	0.171	0.134	0.151

sional differences. For example, the comparisons by season at the bottom of the table show that in the troposphere smallest spectral amplitudes are found during summer in all cases except for meridional wind in Table 1b. The frequency distributions of meridional wind spectral amplitudes (not shown) appear approximately normal during all seasons; as there is no reason to suggest the summer average value is biased by a few very large number, the fact that it does not fit the pattern of the other variables may be ascribed to routine sampling fluctuations.

In addition to the stratifications used earlier, Table 1 includes flight segments over land and ocean, and eastbound and westbound flight segments. Lilly and Petersen (1983) noted a three to six times higher variance at wavelengths greater than 100 km for their four flights over land compared with their 22 flights over water. In Table 1, the variance over land is also greater than the variance over water in all cases. However, the average difference is only about 25 percent. In Table 2, where the spectra were taken over segments 150 km long, this comparison with respect to underlying terrain is focused more sharply by including results over the western United States (104°–122°W). Over this mountainous terrain, the averages range from about two to four times larger than over the ocean.

Airline routing procedures usually attempt to take advantage of the prevailing westerly winds on eastbound flights at midlatitudes, and attempt to avoid headwinds on westbound flights. This bias is seen in Table 1 by the larger mean wind speeds on eastbound, compared with westbound, flights. In no case in Table 1 are the variances significantly different between eastbound and westbound flights, however, suggesting that any dependence of the variance at these scales on background wind speed is too weak to detect with this simple stratification.

Table 2 includes a comparison of the results from east–west and north–south oriented flight segments. The aircraft heading was constrained to be within 20 degrees of north–south or east–west on these segments. Flight direction does not appear to influence the variance of the meridional wind, but the variance of the zonal wind is about forty percent larger on the north–south flights in both the troposphere and stratosphere. While this pattern may be suggestive of anisotropy effects, the small number of flight segments available on the north–south flights render it a tentative result.

The slope of the spectrum across the wavelength range 10–50 km was computed for each of the cases listed in Table 2 by least-squares fitting a straight line to the spectrum in logarithmic coordinates. In all cases with over 40 flight segments, the slopes of the wind components fell between −1.55 and −1.90, and the slope showed no clear dependence on any independent variable. For the case of all flights combined, the slopes of u and v were −1.68 and −1.64 in the troposphere, and −1.76 and −1.68 in the stratosphere, respectively. This analysis supports our earlier suggestion that the slope is near $-\frac{5}{3}$ regardless of season or latitude.

From our analysis the following conclusions can be drawn:

- Velocity and temperature spectra have the same nearly universal shape.

- Spectra of temperature and velocity have slopes close to $-5/3$ for the range of scales between about 2.6 km and 300–400 km. At larger scales the spectra steepen considerably to an approximate slope of -3.
- Spectra show some but not large variations with latitude, season, etc. Potential temperature spectral amplitudes are significantly larger in the stratosphere than in the troposphere. Velocity spectral amplitudes change very little between the troposphere and the stratosphere.
- In the troposphere meridional velocity and potential temperature spectral amplitude is considerably larger at high latitudes than for low latitudes; the variation with latitude of tropospheric zonal velocity is comparatively weak. Also, there is comparatively little variation in spectral amplitude in the stratosphere, at latitudes where there are sufficient data for comparison.
- There is a weak dependence of spectral amplitude with season; especially for tropospheric potential temperature.

In this paper we have presented a description of the major features evident in the GASP wavenumber spectra. A companion paper (Gage and Nastrom, 1985) addresses the theoretical interpretation of the observed spectra.

Acknowledgment. The research reported in this paper has been supported in part by the GARP Office of the National Science Foundation.

REFERENCES

Atkinson, B. W., 1981: *Meso-Scale Atmospheric Circulations,* Academic Press, Chap. 1.

Balsley, B. B., and D. A. Carter, 1982: The spectrum of atmospheric velocity fluctuations at 8 km and 86 km. *Geophys. Res. Lett.,* **9,** 465–468.

Boer, G. J., and T. G. Shepherd, 1983: Large-scale two-dimensional turbulence in the atmosphere. *J. Atmos. Sci.,* **40,** 164–184.

Brown, P. S., and G. D. Robinson, 1979: The variance spectrum of tropospheric winds over Eastern Europe. *J. Atmos. Sci.,* **36,** 270–286.

Charney, J. G., 1971: Geostrophic turbulence. *J. Atmos. Sci.,* **28,** 1087–1095.

Chen, T. C., and A. Wiin-Nielsen, 1978: On nonlinear cascades of atmospheric energy and enstrophy in a two-dimensional spectral index. *Tellus,* **30,** 313–322.

Dewan, E. M., 1979: Stratospheric spectra resembling turbulence. *Science,* **204,** 832–835.

Gage, K. S., 1979: Evidence for a $k^{-5/3}$ law inertial range in mesoscale two-dimensional turbulence. *J. Atmos. Sci.* **36,** 1950–1954.

——, and G. D. Nastrom, 1985: Theoretical interpretation of atmospheric wavenumber spectra observed during GASP. Submitted to *J. Atmos. Sci.*

Fiedler, F., and H. A. Panofsky, 1970: Atmospheric scales and spectral gaps. *Bull. Amer. Meteor. Soc.,* **51,** 1114–1119.

Garrett, C., and W. Munk, 1979: Internal waves in the ocean. *Annual Reviews in Fluid Mechanics,* Vol. 11, Annual Reviews, 339–369.

Kao, S. K., and L. L. Wendell, 1970: The kinetic energy of the large-scale atmospheric motion in wavenumber-frequency space. I: Northern Hemisphere. *J. Atmos. Sci.,* **27,** 359–375.

Larsen, M. F., M. C. Kelley and K. S. Gage, 1982: Turbulence spectra in the upper troposphere and lower stratosphere between 2 hours and 40 days. *J. Atmos. Sci.,* **39,** 1035–1041.

Lilly, D. K., 1983: Stratified turbulence and the mesoscale variability of the atmosphere. *J. Atmos. Sci.,* **40,** 749–761.

——, and E. Petersen, 1983: Aircraft measurements of atmospheric energy spectra. *Tellus,* **35A,** 379–382.

Nastrom, G. D., and K. S. Gage, 1983: A first look at wavenumber spectra from GASP data. *Tellus,* **35A,** 383–388.

——, and W. H. Jasperson, 1983: Flight summaries and temperature climatology at airliner cruise altitudes from GASP data. NASA CR-168106, 368 pp. [Available from NTIS; N83-24048/1.]

——, K. S. Gage and W. H. Jasperson, 1984: The atmospheric kinetic energy spectrum, 10^0–10^4 km. *Nature,* **310,** 36–38.

Olbers, D. J., 1983: Models of the oceanic internal wave field. *Rev. Geophys. Space Phys.,* **15,** 1567–1606.

Papathakos, L. C., and D. Briehl, 1981: NASA Global Atmospheric Sampling Program (GASP) data report for tapes VL0015, VL0016, VL0017, VL0018, VL0019, and VL0030. *NASA-TMX-81661,* 94 pp.

Perkins, P. J., 1976: Global measurements of gaseous and aerosol trace species in the upper troposphere and lower stratosphere from daily flights of 747 airliners. *NASA-TMX-73544,* 23 pp.

Stickney, T. M., N. W. Shedlov, D. I. Thomson and F. J. Yakos, 1981: Rosemount total temperature sensors. Tech. Rep. 5755, Rosemount Inc., Minneapolis, MN.

Tang, C. M., and S. A. Orszag, 1978: Two-dimensional turbulence on the surface of a sphere. *J. Fluid Mech.,* **87,** 305–319.

VanZandt, T. E., 1982: A universal spectrum of buoyancy waves in the atmosphere. *Geophys. Res. Lett.,* **9,** 575–578.

Vinnichenko, N. K., 1970: The kinetic energy spectrum in the free atmosphere −1 second to 5 years. *Tellus,* **22,** 158–166.